J Electr Eng Technol.2018; 13(5): 1807-1813
http://doi.org/10.5370/JEET.2018.13.5.1807

ISSN(Print) 1975-0102
ISSN(Online) 2093-7423

Single Line-to-ground Fault Location and Information Modeling Based on the Interaction between Intelligent Distribution Equipment

Lei Wang*, Wei Luo†, Liangjie Weng, Yongbo Hu** and Bing Li*****

Abstract – In this paper, the fault line selection and location problems of single line-to-ground (SLG) fault in distribution network are addressed. Firstly, the adaptive filtering property for empirical mode decomposition is formulated. Then in view of the different characteristics showed by the intrinsic mode functions(IMF) under different fault inception angles obtained by empirical mode decomposition, the sign of peak value about the low-frequency IMF and the capacitance transient energy is chosen as the fault line selection criteria according to the different proportion occupied by the low-frequency components. Finally, the fault location is determined based upon the comparison result with adjacent fault passage indicators' (FPI) waveform on the strength of the interaction between the distribution terminal unit(DTU) and the FPI. Moreover, the logic nodes regarding to fault line selection and location are newly expanded according to IEC61850, which also provides reference to acquaint the DTU or FPI's function and monitoring. The simulation results validate the effectiveness of the proposed fault line selection and location methods.

Keywords: Empirical mode decomposition, Fault line selection, Fault locating, IEC61850, Small-current grounding fault.

1. Introduction

Power outage incidents are commonly caused by the fault in the distribution network. The access of power distribution system (PDS) needs to construct intelligent distribution network all point out in order to improve the reliability of residential electricity consumption. However, for a mass of distribution equipment, such as DTU and FPI, the traditional communication protocol (for example the IEC60870-5 series) can't describe the complex instructions and information. The IEC61850 is recognized as the most suitable communication protocol for PDS and is especially applied to fault line selection or location.

The DTU or FPI is generally used to solve the SLG fault selection and location. The DTU is expensive but functional and cannot be used in large doses. The FPI is just the opposite. The characteristics obtained by the DTU have been focused by many researchers like O Chaari, G Song [1-4] to find the fault line or the fault selection, but they did not solve the problem completely. The PDS is complicated with different fault times, sections and resistances all leading to different transient components. Moreover, the uncertain interfering noise is also a difficult challenge for the traditional methods that relay on fixed frequency filter algorithm or the direction of the fault. As for FPI, a method using Zigbee has been proposed in [5]. However, this method is unable to support IEC61850 due to high cost of FPI. Thus, [6-7] provide some references about how to use FPI in fault location and make the FPI support IEC61850.

Considering the above-mentioned problems, this paper proposes a new method to solve the problem of SLG's fault selection and location based on the interaction between the DTU and the FPI. The remaining of this paper is organized as follows: Section 2 and 3 discuss an adaptive filtering property for empirical mode decomposition that is formulated to analyze the transient component of fault line selection; In section 4, the method about finding the fault sections is proposed based upon the interaction between the DTU and the FPI. The logical nodes about fault line selection and FPI monitoring are presented in section 5 that enable the FPI to support IEC61850. Finally, the simulation results verifying the feasibility and validity of the proposed method are provided in section 6 followed by conclusion in section 7.

2. The Features of Empirical Mode Decomposition

The empirical mode decomposition was proposed as a new type of adaptive signal time-frequency analysis method by N. E. Huang [8] in 1998. In empirical mode decomposition, the signals of different frequency band called IMFs are just obtained from the characteristics of the signal itself. Large number of engineering practices has

† Corresponding Author: State Grid Anhui Electric Power Company Anhui Maintenance Company, China. (luowei@mail.hfut.edu.cn)
* Anhui New Energy Utilization and Energy Saving Laboratory (Hefei University of Technology), China. (Lwang_hf@126.com)
** State Grid Anhui Electric Power Company Anhui Maintenance Company, China.
*** State Grid Anhui Electric Power Company Hefei Power Supply Company, China.
Received: April 9, 2017; Accepted: April 23, 2018

already confirmed the empirical mode decomposition as a powerful tool for nonlinear fault waveform analysis that has similar characteristics of binary filtering. Moreover, the characteristics of empirical mode decomposition are local self-adaptive, which is embodied in detection of instantaneous frequency.

The signal $\hat{x}(t)$ is obtained from the Hilbert transform of $x(t)$, so analytical signal $z(t)$ can be expressed as:

$$z(t) = x(t) + j\hat{x}(t) = a(t)\,\mathrm{e}^{j\theta(t)} \tag{1}$$

Where $a(t)$ is the amplitude function and $\theta(t)$ is the Phase function. The instantaneous frequency $f_i(t)$ can be expressed as:

$$f_i(\mathrm{t}) = \frac{1}{2\pi}\cdot\frac{d\theta(\mathrm{t})}{dt} \tag{2}$$

Different from the triangle decomposition, $f_i(t)$ obtained from the Hilbert transform is local component. Thus, $x(t)$ as a multi-component signal can be expressed as:

$$x(\mathrm{t}) = \sum_{i=1}^{N} c_i(\mathrm{t}) + r(\mathrm{t}) \tag{3}$$

where $c_i(t)$ and $r(t)$ are the single-component signal and the residual signal, respectively. Getting single-component signals is the key to obtain the instantaneous frequency. Differing from the Fourier decomposition using triangle basis as time scale, the implied local-oscillation scale is adopted creatively with empirical mode decomposition [9]. Correspond to formula (3), the original signal is decomposed into multiple narrow-band components (i.e., the IMF). Firstly, such process avoids defining the local average time scales, meanwhile only the instantaneous frequency defined in the IMF has specific physical meaning. Secondly, the empirical mode decomposition does not require predefined basis function or any prior knowledge. Therefore, this algorithm has excellent adaptability.

The empirical mode decomposition divides the original signal into several IMF and a remaining signal:

$$s(t) = \sum_{i=1}^{n} IMF_i(t) + r(t) \tag{4}$$

The IMF has different characteristic time scales that can obtain the instantaneous frequency resolution by:

$$\Delta f_i = \frac{f_{i\max}}{N} \tag{5}$$

Due to local self-adaptive, each IMF can express multiple dominant frequencies according to the actual waveform characteristics and it all caused by the fault. This is the most significant difference between the empirical mode decomposition and the algorithm merely based on the harmonic signal analysis. The empirical mode decomposition can be regarded as an intelligent band-pass filter, whose cut-off frequency and bandwidth are selected by the physical significance of the signal.

3. The Application of Empirical Mode Decomposition

3.1 Transient current character of SLG fault

Arc suppression coil used in the PDS effectively suppresses the fault current, but the difficulty of fault line selection is increased. The compensation of arc suppression coil makes phase of the current and the zero-sequence voltage almost unanimous. Therefore, it is difficult to select the fault line with only the fault parameters at steady-state captured by the DTU. However, the fault transient process contains the abundant fault information that can be used as line selection criterions. The improvement of the DTU technology has made it possible to capture intact and accurate capacitance transient current waveform.

When SLG fault happens, the transient component of fault current is mainly caused by the sudden increase of fault phase voltage, which is made up of capacitance transient current and low-frequency inductor current. [10] provide the formula of transient current:

$$\begin{aligned} i_0 &= i_{st} + i_{os} = i_L + i_C = (I_{Cm} - I_{Lm})\cos(\omega\mathrm{t}+\varphi) \\ &+ I_{Lm}\cos\varphi e^{\frac{-t}{\tau_L}} + I_{Cm}(\frac{\omega_f}{\omega}\sin\varphi\sin\omega\mathrm{t} - \cos\varphi\cos\omega_f t)e^{\frac{-t}{\tau_C}} \end{aligned} \tag{6}$$

where φ is the fault inception angle, τ_L and τ_C are the decay time constants for the line inductance and capacity, I_{Lm} and I_{Cm} are the amplitude current for the line inductance and capacity, respectively, and ω_f is the angular frequency of transient free oscillation component.

According to the above formula, the attenuation high-frequency component changes along with the fault inception angle. In view of fault vibration and noise pollution, the transient component will be more complex. Therefore, various signal analysis methods like wavelet face the following problems: the selection of base is sensitive and difficult; in the case of small fault inception angle, the method is inaccurate due to the lack of high-frequency component.

3.2 Fault line selection base on empirical mode decomposition

The empirical mode decomposition is similar to a low-pass filter. The local frequency declines with increase in the IMF level resulting in different characteristic

frequency waveform. The empirical mode decomposition also contains excellent completeness, via HHT (Hilbert Huang Transform) the IMF can obtain the instantaneous frequency that has physical meaning to analysis about uncertain factors of complex power network fault.

Firstly, in the situation of SLG fault with small fault inception angle, the high frequency component of the fault line is reduced, while the current inception direction obviously opposite than others. Secondly, in case of large fault inception angle, although the current inception direction cannot be used as a criterion, the high-frequency transient component is much more than the power frequency component and the noise superposition. Meanwhile, the zero-sequence fault current is supplied by the point of failure, so the fault line's capacitance transient energy is the sum of other lines.

Based on the above-mentioned two points, the SLG fault selection method is obtained and described below.

Apply the empirical mode decomposition to each line's fault currents and then through FFT find different IMFs gradually reducing the core-frequency. The high-frequency capacitance transient current component, the fault noise and the low-frequency fundamental current component are adaptively decomposed in different IMFs. Set the core-frequency less than 50 Hz as the low-frequency IMFs. The low-frequency transient energy ratio P can be expressed as:

$$P = \frac{\sum_{i=1}^{n} (\sum IMF_{low}(i) + r(i))^2}{\sum_{i=1}^{n} (\sum IMF_{all}^2(i)^2 + r^2(i))} \tag{7}$$

The larger P is, the more low-frequency transient energy contents. IMFlow is the sum of IMFs with core frequency below 50 Hz and IMFall is the sum of all IMFs. Given the weakness about aliasing of the empirical mode decomposition, the low-frequency transient energy obtained from formula is usually lower than the actual one. Therefore, the threshold value of P is set as 0.3 as reliable criterion.

When fault occurs, the fault currents are sufficient of capacitance transient energy if the low-frequency transient energy ratio of every line is less than the threshold. Thus, the IMFs with core frequency between the attenuation capacitance-frequency are summed and called IMFc. The capacitance transient energy Ec can be expressed as:

$$E_c = \| IMF_c(n) \|^2 \tag{8}$$

The Ec of fault line should be greater than that of non-fault lines'.

However, the power frequency is relatively obvious if the P of the most lines is higher than the threshold. The high-frequency interference signals can be filtered using the characteristics of the adaptive filter. At the same time, the empirical mode decomposition is sensitive to singular point. There is an extreme value point coming out at fault time, so the sign of peak value pointing near the fault time can substitute the direction of fault phase. Thus, the sign of fault line is opposite to non-fault lines'.

4. The Interaction between DTU and FPI

Making DTU as FPIs' concentrator and using the FPIs to find the fault section is the best method to use with this distribution automation equipment. Using the above-mentioned method, the DTU can set the related parameters such as fault setting for FPI, and the logical node of FPI monitoring properties can also be integrated into DTU's self-describing files that can solve the problem of FPI of IEC61850 protocol support.

The interaction between the DTU and the FPI is ascribed to the following steps: when fault occurs, the master station receives the failure data of line selection from the DTU and return the fault line though the proposed fault line selecting method; then the DTU of fault line inform the FPIs on its line to start work; FPIs upload the fault information to the DTU, the DTU obtains the fault section using the fault line locating method and uploads it to the master station.

There are a number of different criterions of FPI used for fault location. In addition to the traditional over current or transient current detection, waveform similarity comparison about the steady-state fault current obtained from FPI is presented to locate the fault section.

The time when the SLG fault happens, the compensation of arc suppression coil results in fault current that is greater than the attenuation zero-sequence one between the adjacent FPIs and flows to the branch that is connected with the distribution transformer. Moreover, the similarity between the adjacent FPIs in fault place has certain differences compared with others.

In order to reduce the data transmission pressure, the low-frequency amplitude is obtained from FFT instead of the using the complete sampling signal for contrasting. The first nine harmonics called x_n (n = 0... 9) obtained by FPIs can be seen as characterization of waveform. The similarity degree S can be obtained by uploading these harmonics to the DTU and is expressed as:

$$S[j] = \sum_{n=0}^{9} \sqrt{(x_n^i - x_n^{i-1})^2} \tag{9}$$

Where i and j denote the ith FPI on the jth line. In order to offset line attenuation effect while judging the fault section, singularity analysis is used on *S*. If *S* contains an obvious peak, the fault location can be determined. Finally, the DTU uploads fault location by IEC61850.

Generally cause the function of wave record DTU sampling rate is more than 10kHZ, so according to the criterion about the current or the system voltage the time of failure can be quickly judged (less than 1 ms). However,

the FPI sampling rate is low, usually less than 1kHZ, and the normal transmission rate of ZigBee is about 40 Kbps, response time is 25ns which far less than FPI sampling rate, thus response time of DTU and FPI interaction does not affect the FPI Startup synchronization rate.

5. Logical Node of Fault Location

The FPI is usually unable to support the IEC61850. However, the DTU can take advantage of commanding them by making the FPI as part of the DTU. The class for this function is a must. At the same time, there is no associated class of SLG fault defined in IEC61850. Therefore, a class must be extended following the protocol in order to use the function of fault location through IEC61850[11-12].

The class of SLG fault line selection and location is shown in Table 1. The PSEF (selection of single-phase earthling fault) contains most of the useful logical nodes through the empirical mode decomposition and all the decomposition information node data is inherited from common logical node class.

In view of the FPI monitoring, the class named SWPI (waveform parameters indicator) shown in Table 2 is containing EEHealth and WavHmv for commanding FPI and for recording the measurements of the FPI, respectively. Other functions can be expanded as required.

Table 1. Class for the small-current grounding fault line selection containing the empirical mode

PSEF class				
Data object name	Common data class	Explanation	T	M/O
LNName		Shall be inherited from logical-node class (see IEC 61850-7-2)		M
DATA				
System logical node data				
LN shall inherit all mandatory data from common logical node class				M
Status information				
Str	ACD	Start		M
Op	ACT	Operation		O
FltFedID	INS	The ID number of fault line		M
Measured values				
TransVclc	MV	Transient zero-sequence voltage		O
TransAclc[n]	MV	Transient zero-sequence fault current		O
EIMF[n]	MV	The energy of every IMF		O
SigPeakV[n]	MV	Sign of peak value		M
TranPro [n]	MV	Low-frequency transient energy ratio		M
TranEngC[n]	MV	Capacitance transient energy		M
Settings				
TranProLow	ASG	Minimum threshold of low-frequency transient energy ratio		M
OSHigh	ING	Upper frequency of capacitance transient		M
OSLow	ING	Low frequency of capacitance transient		M

Table 2. Class for the steady-state fault waveform comparison

SWPI class				
Data object name	Common data class	Explanation	T	M/O
LNName		Shall be inherited from logical-node class (see IEC 61850-7-2)		M
DATA				
System logical node data				
LN shall inherit all mandatory data from common logical node class				M
Status information				
EEHealth	SI	Healty of FPI		O
Measured values				
WavHmv[n]	HMV	Harmonic component of FPI		O
Measured values				
Wavmut	ASG	Number of sudden changes waveforms		M
NumFPI	NG	Number of FPI		M
FPIName[n]	ObjectName	Name of FPI		M

Table 3. Class for the small-current location

RSEF class				
Data object name	Common data class	Explanation	T	M/O
LNName		Shall be inherited from logical-node class (see IEC 61850-7-2)		M
DATA				
System logical node data				
LN shall inherit all mandatory data from common logical node class				M
Status information				
EEHeaklth	ISI	Healty of function		
Settings				
FltFedID	INS	Number of fault line		M
FltFPIID	INS	Number of FPI of fault section		M
FltAlm	SPS	Fault alarm		M

RFLO as a class of fault location has been defined in IEC61850, but it cannot be applied to the proposed method. Therefore, RSEF (the location of single phase earthing fault) is presented as Table 3.

6. Simulation Verification and Analysis

6.1 Simulation model

In order to validate the feasibility of the proposed fault location method, Matlab/simulink is used to set a model of SLG fault as shown in Fig. 1 In this PDS, the arc suppression coil is used for overcompensation that is set as 8%. The lengths of four lines are given as 3km, 6km, 10km and 10km, respectively. The fault is set to happen at 5km of the third line and the interval of the FPI is set as 500m based on the Zigbee network.

6.2 Data analysis about SLG fault

The fault time is set as 0.01s and the zero-sequence

Table 4. The ratio of low-frequency energy under different fault inception angles in each line

Number of line	P at 0°	P at 15°	P at 30°	P at 60°	P at 90°
1	0.8157	0.4826	0.2663	0.1865	0.1732
2	0.8022	0.387	0.2661	0.1179	0.1646
3	0.4239	0.4089	0.1749	0.1042	0.0757
4	0.6867	0.4951	0.1681	0.1963	0.2327

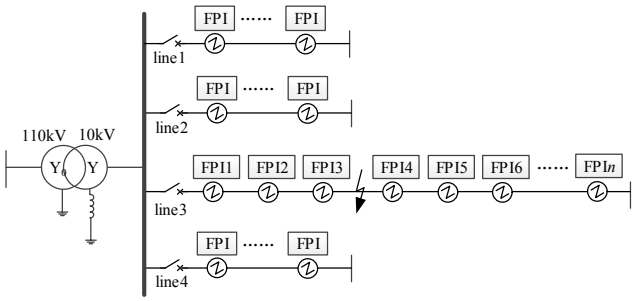

Fig. 1. Diagram of the small current grounding fault Simulation

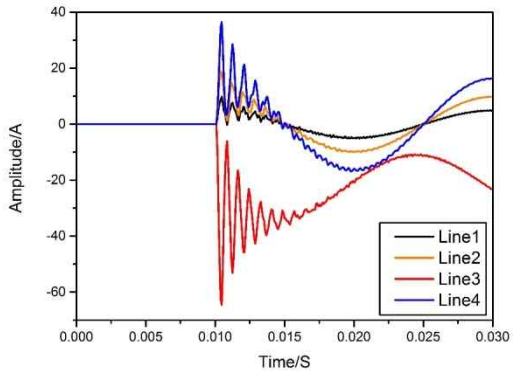

(a) The line waveform

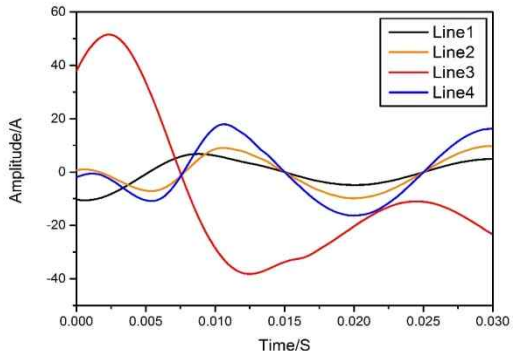

(b) Low-frequency waveform of short circuit

Fig. 2. Waveforms of the line and the low-frequency under the fault inception angle 0°.

current between the half power frequency before fault and a period after the fault of all lines is obtained. The empirical mode decomposition and formula (7) are used to obtain the low-frequency transient energy ratio P. Then the angle of the fault is changed. The steps are repeated and peat such steps and the data is shown in table 4.

Table 5. Low-frequency fault direction under the fault inception angle 0°

Number of line	the sign of peak value	Time of maximum amplitude (ms)	Time of minimum amplitude (ms)
1	Max	8.9	20.1
2	Max	10.6	20.0
3	Min	2.4	12.5
4	Max	10.7	20.0

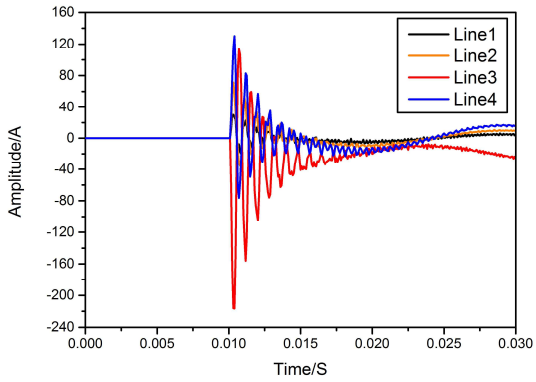

(a) The line waveform

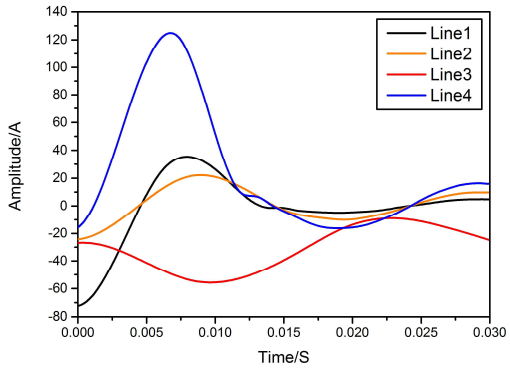

(b) Low-frequency waveform of short circuit

Fig. 3. Waveforms of the line and the low-frequency under the fault inception angle 15

According to the data in table 4, it can be proved that with the increase of fault inception angle, the transient energy of the high frequency component becomes larger, so the value of P decrease gradually.

According to above description, the sign of the peak value can be selected as criterion of the fault inception angle whose minimum P value is smaller than 0.3.

Fig. 2 shows the waveform at fault inception angle 0°, and after the empirical mode decomposition algorithm filter out high frequency component of low-frequency waveform.

Contrast Fig. 2 (a) and (b), compared with other paper the method thought empirical mode decomposition algorithm can get low frequency component more accurately, at the same time, the wave phase of line3 is contrary to other lines which prove the proposed criterion, comply with the

above analysis analyze the data and the results as shown in table 5.

Similarly, Fig. 3 shows the waveform at fault inception angle 15°, and after the empirical mode decomposition algorithm filters out the high frequency component of low-frequency waveform.

In Fig. 3, the direction of the fault line's singular point is near the fault time (10ms), which is contrary to others too. Thus, line 3 can be determined as the fault line.

Analyze the data and the results as shown in Table 6.

At other fault inception angles, P is less than 0.3. Therefore, capacitance transient energy Ec is used as the criterion and table 7 is obtained.

In table 7, cause line 3 collects all capacitance transient energy, which is greater than others and proves the accuracy of the proposed criterion. Considering that the PDS is usually manifest as radiant and multiple stages, the transient component becomes more obvious with increasing the number of lines.

Waveform obtained from fault inception angle 0 °, 15 °, 30 °, 60 °, 90 °is analyzed above, according to this, the data of table 5, table 6 and table 7 is calculated. Through the comparison of data with different criterions, the line 3 is verified as the fault line under different fault inception angles, which conforms with the result of simulation.

After the fault line is selected by the above method, the FPI of fault line is started. Adjacent six FPI on the line 3 are selected as simulation target. The fault steady zero-sequence current is obtained and 0 ~ 9 times harmonic data is calculated as shown in Table 8.

In Table 8, thought the harmonics gradually decreased, the fault location can not get. Then similarity degree S is obtained through the formula (9)

$$S = [\,0.271 \quad 0.271 \quad 2.07 \quad 0.273 \quad 0.274];$$

S[3] is about 10 times bigger than other numbers. Hence, the fault can be determined to occur between 3rd and 4th FPI, which prove that the simulation result is correct.

Table 6. Low-frequency fault direction under the fault inception angle 15°

Number of line	the sign of peak value	Time of maximum amplitude (ms)	Time of minimum amplitude (ms)
1	Max	8.0	19.1
2	Max	9.0	19.4
3	Min	22.9	9.7
4	Max	6.8	18.9

Table 8. Harmonic component with FPI

Harmonic times	FPI1 (A)	FPI2 (A)	FPI3 (A)	FPI4 (A)	FPI5 (A)	FPI6 (A)
0	0.2399	0.2397	0.2395	0.0002	0.0002	0.0000
1	5.3381	5.0673	4.7968	2.9989	2.7263	2.4540
2	0.0092	0.0092	0.0092	0.0000	0.0000	0.0003
3	0.0061	0.0061	0.0061	0.0001	0.0000	0.0003
4	0.0046	0.0046	0.0046	0.0001	0.0000	0.0003
5	0.0037	0.0036	0.0037	0.0001	0.0000	0.0002
6	0.0030	0.0030	0.0031	0.0001	0.0000	0.0002
7	0.0026	0.0026	0.0026	0.0001	0.0000	0.0002
8	0.0023	0.0023	0.0023	0.0001	0.0000	0.0002
9	0.0020	0.0020	0.0020	0.0001	0.0000	0.0002

7. Conclusion

The growing requirements of the distribution network reliability have rapidly increased the development of intelligent electronic equipment. In this paper, the adapt-ability of empirical mode decomposition is used in SLG fault line selection and a new method is proposed that make the FPI to cooperate with the DTU to find the fault section. Then the logical node about relevant method is expanded following the IEC61850, which also solve the problem of the support of

FPI's communication. The proposed method is combined with the new development direction of distribution network automation communication providing a feasible scheme for the perfection of the distribution network automation that has been demonstrated by the simulation results.

In summary, the original contributions of current research include 1)using empirical mode decomposition in pre-processing of fault current and getting the low-frequency waveform and the low-frequency transient energy of short circuit, 2) exploiting low- frequency transient energy ratio to selecting criteria for selecting the fault lines, 3)calculating the low-frequency fault direction from low-frequency waveform and the capacitance transient energy form IMFc, through them to determine the fault line, 4) calculating the similarity degree offset line attenuation effect and judging the fault section, 5) exploring the interaction between DTU and FPIs and demonstrate its feasibility, 6) expanding the logic nodes regarding to fault line selection and location according to IEC61850, which provides reference to acquaint the DTU or FPI's function and monitoring.

Table 7. The capacitance transient energy and its core frequency under different fault inception angles in each line

Number of line	30°		60°		90°	
	Capacitance transient energy	Core frequency (Hz)	Capacitance transient energy	Core frequency (Hz)	Capacitance transient energy	Core frequency (Hz)
1	215.5	2400 1200	10800	800 1200 2400	66125	800 1200 2400
2	28700	2400 1200	51000	2400 1200	296570	2400 1200
3	266000	1200	435000	1300 1250	3473200	2400 1200
4	33200	1200 2400	154000	2400 1200	1047500	1250 2400

References

[1] A. Borghetti., M. Bosetti, D.M. Silvestro and et al, "Continuous-Wavelet Transform for Fault Location in Distribution Power Networks: Definition of Mother Wavelets Inferred From Fault Originated Transients," *IEEE Transactions on Power Systems*, vol. 23, no. 2, pp. 380-388, 2008.

[2] G.Song., Z.Ma., G.Li and et al, "Phase current fault component based single−phase earth fault segment location in non-solidly earthed distribution networks," *International Transactions on Electrical Energy Systems*, vol. 25, no. 11, pp. 2713-2730, 2016.

[3] H. Nouri, M. M. Alamuti, "Comprehensive Distribution Network Fault Location Using the Distributed Parameter Model," *IEEE Transactions on Power Delivery*, vol. 26, no. 4, pp. 2154-2162, 2011.

[4] M. Pourahmadi-Nakhli, A. A. Safavi, "Path Characteristic Frequency-Based Fault Locating in Radial Distribution Systems Using Wavelets and Neural Networks," *IEEE Transactions on Power Delivery*, vol. 26, no. 2, p. 772-781, 2011.

[5] P. Yi, A. Iwayemi, C. Zhou. "Developing ZigBee Deployment Guideline Under WiFi Interference for Smart Grid Applications." *IEEE Transactions on Smart Grid*, vol. 2, no. 1, pp. 110-120, 2011.

[6] J.H.Teng, W.H.Huang, S.W.Luan, "Automatic and Fast Faulted Line-Section Location Method for Distribution Systems Based on Fault Indicators," *IEEE Transactions on Power Systems*, vol. 29, no. 4, pp. 1653-1662, 2014.

[7] R. Ma, H.H. Chen, R.Y. Huang and et al, "Smart Grid Communication: Its Challenges and Opportunities," *IEEE Transactions on Smart Grid*, vol. 4, no. 1, pp. 36-46, 2013.

[8] N.E. Huang, Z. Wu, "A review on Hilbert−Huang transform: Method and its applications to geophysical studies," *Reviews of Geophysics*, vol. 46, no. 2, RG2006, 2008.

[9] M. Feldman, "Time-varying vibration decomposition and analysis based on the Hilbert transform," *Journal of Sound & Vibration*, vol. 295, no. 3, pp. 518-530, 2006.

[10] F. ZHANG, Z.C.PAN, H.ZHANG, et al. "New Criterion of Fault Line Selection in Non-Solidly Earthed Network Based on the Maximum of Zero Sequence Transient Current," *Automation of Electric Power Systems*, 30, no. 4, pp. 45-48, 2006.

[11] S.T. Sidhu, Y. Yin, "Modelling and Simulation for Performance Evaluation of IEC61850-Based Substation Communication Systems," *IEEE Transactions on Power Delivery*, vol. 22, no. 3, pp. 1482-1489, 2007.

[12] G. Zhabelova and V. Vyatkin, "Multiagent Smart Grid Automation Architecture Based on IEC 61850/61499 Intelligent Logical Nodes," *IEEE Transactions on Industrial Electronics*, vol. 59, no. 5, pp. 2351-2362, 2012.

Lei Wang received the Ph.D. degree in electrical engineering from University of Chinese Academy of Sciences, Beijing, China, in 2010. He is currently an Associate Professor at the School of Electrical Engineering and Automation, Hefei University of Technology. His research interests are in the distribution automation, distributed generation and Micro-grid.

Wei Luo received the M.S. degree in electrical engineering from Hefei University of Technology, Hefei, China, in 2016, Currently, He is currently serve at State Grid Anhui Electric Power Company Anhui Maintenance Company. His research interests are in the distribution automation and distribution reliability.

Liangjie Weng received the B.S. degree in electrical engineering from Shanghai Electric Power University, Shanghai, China, in 2006, Currently, He is currently serve at State Grid Anhui Electric Power Company Anhui Maintenance Company. His research interests are in distribution automation and UHV technology.

Yongbo Hu received the B.S. degree in electrical engineering from University of Anhui, Hefei China, in 2009, Currently, He is currently serve at State Grid Anhui Electric Power Company Anhui Maintenance Company. His research interests are in distribution automation and Relay protection.

Li Bing received the M.S. degree in electrical engineering from Huazhong University of Science and Technology, Wuhan, China, in 2006. He is currently serve at the State Grid Anhui Electric Power Company Hefei Power Supply Company. His research interests are in the distribution automation and power line operation maintenance.